Effect of degree of saturation on stresses and pore water pressure in the subgrade layer caused by railway track loading

Mohammed Y. Fattah
Department of Civil Engineering, UOT, Baghdad, Iraq
Qutaiba G. Majeed
Department of Civil Engineering, Diyala University, Diyala, Iraq, and
Hassan H. Joni
Department of Civil Engineering, UOT, Baghdad, Iraq

Received 24 April 2024
Revised 12 June 2024
Accepted 13 June 2024

Abstract

Purpose – The experiments of this study investigated the effect of the subgrade degree of saturation on the value of the stresses generated on the surface and the middle (vertical and lateral stresses). The objectives of this study can be identified by studying the effect of subgrade layer degree of saturation variation, load amplitude and load frequency on the transmitted stresses through the ballast layer to the subgrade layer and the stress distribution inside it and investigating the excess pore water pressure development in the clay layer in the case of a fully saturated subgrade layer and the change in matric suction in the case of an unsaturated subgrade layer.

Design/methodology/approach – Thirty-six laboratory experiments were conducted using approximately half-scale replicas of real railways, with an iron box measuring 1.5 x 1.0 × 1.0 m. Inside the box, a 0.5 m thick layer of clay soil representing the base layer was built. Above it is a 0.2 m thick ballast layer made of crushed stone, and on top of that is a 0.8 m long rail line supported by three 0.9 m (0.1 × 0.1 m) slipper beams. The subgrade layer has been built at the following various saturation levels: 100, 80, 70 and 60%. Experiments were conducted with various frequencies of 1, 2 and 4 Hz with load amplitudes of 15, 25 and 35 kN.

Findings – The results of the study demonstrated that as the subgrade degree of saturation decreased from 100 to 60%, the ratio of stress in the lateral direction to stress in the vertical direction generated in the middle of the subgrade layer decreased as well. On average, this ratio changed from approximately 0.75 to approximately 0.65.

Originality/value – The study discovered that as the test proceeded and the number of cycles increased, the value of negative water pressure (matric suction) in the case of unsaturated subgrade soils declined. The frequency of loads had no bearing on the ratio of decline in matric suction values, which was greater under a larger load amplitude than a lower one. As the test progressed (as the number of cycles increased), the matric suction dropped. For larger load amplitudes, there is a greater shift in matric suction. The change in matric suction is greater at higher saturation levels than it is at lower saturation levels. Furthermore, it is seen that the load frequency value has no bearing on how the matric suction changes. For all load frequencies and subgrade layer saturation levels, the track panel settlement rises with the load amplitude. Higher load frequency and saturation levels have a greater impact.

Keywords Subgrade clay, Unsaturated, Track, Matric suction, Stresses

Paper type Research paper

Railway Sciences
Vol. 3 No. 4, 2024
pp. 413-436
Emerald Publishing Limited
e-ISSN: 2755-0915
p-ISSN: 2755-0907
DOI 10.1108/RS-04-2024-0011

1. Introduction

The improvement and advancing in the technology of transportation and the requirement of efficiency for goods transportation and mobility of passengers make the railway track regularly needed to carry higher loading at higher speeds. It ends up important that the conduct of track foundation subgrade under cyclic and dynamic loading conditions be completely captured, so, during the design phase and in-service phase, the impacts of new traffic loading attributes can be thought about.

In the ballasted railway track, the load of trains carriage is dispersed and transmitted by means of the rails to the sleepers and then through to ballast and subballast; finally, the load is spread onto the subgrade. The subgrade soil layer characteristics administer the value of stress that can be subjected to the subgrade layer. In fine-grained subgrade, the applying of high magnitudes of loading and frequency will cause an increase in strain accumulation, the build-up of excess pore water pressure in saturated soil and a matric suction effect in the case of unsaturated subgrade soil. This may lead to concern about the safety and stability of railways.

In the field, the subgrade soil is frequently unsaturated and subjected to continuous varieties in degree of temperature, water content and suction (Jin, Lee, & Kovacs, 1994; McCartney & Khosravi, 2013). Numerous studies of experimental and theoretical approaches (François & Laloui, 2008; Uchaipichat & Khalili, 2009; Wu & Shi, 2023) stated that partially saturated soils behavior depends mainly on both suction and degree of temperature.

Increases in strength and stiffness of the soil probably take place according to the value of the suction. It was found by Gräbe (2002) that the stiffness obtained in the laboratory was lower than that back-calculated from field observation for saturated specimens replicating railway formation. It was presumed that this may be due to the effect of suction in the field. Hence, research is required to understand the impact of suction and its variation on the behavior of railway subgrade, consequently leading to more clear comprehension of in-situ soil behavior. Generally, the concentration of these studies was on the cases of monotonic behavior of the soils that are loaded with more than 1% strains. At small strains (less than 1%) and various degrees of temperature, partially saturated soils cyclic behavior is particularly not fully understood (Chao, 2014).

The main purpose of subgrade is by considering it as a foundation that supports the track. Practically, it should be qualified (Chandra & Agarwal, 2007):

(1) To serve as working base for the built ballast and subballast.

(2) To support track structure.

(3) To accommodate the stresses due to loads.

(4) To easy the drainage processes.

The effect of wheel loads can reach a depth of many meters below the ties in spite that the loads decrease in the subgrade through distribution from the superstructure, ballast and subballast. Therefore, the subgrade in this zone should be able to resist the loads and extra deformation that are caused by the wheel loads and self – weight of the track and substructure. Additionally, a strong floor should be provided with time, and it should not be extremely sensitive to environmental conditions. Also, easy drainage for the groundwater should be kept in mind during the design stage of the subgrade.

Subgrade may be exposed to overstresses that are known as cumulative plastic deformation and progressive shear failure due to repeated wheel loads. These two failure modes are considered the main types of subgrade failure when it contains fine – grain cohesive soil. These may cause degradation of track geometry conditions and then increase the dynamic loads of the wheel. Despite the fact that the soft subgrade is more experienced

with deterioration, the hard subgrade is also probably subject to deterioration. In hard subgrade, the main problem is erosion, which is caused by coarse ballast grain with the existence of water. This may lead to erosion of fine material and cause ballast fouling and reduce its permeability, which influence track life, capability and maintenance requirements.

The load factor is considered an external factor, and it depends on self – weight of the track and repeated wheel loads. The self – weight of track is the main cause of massive shear failure and consolidation problems. Repeated loads will cause the essential failure type of subgrade, which includes progressive shear failure and excessive plastic deformation. There is a difference between the subgrade behavior with the stationary loads and cyclic loads due to (Li, Sussmann, Hyslip, & Chrismer, 2016):

(1) Soil of fine particles has less resistance under cyclic loads than static loads of the same value.

(2) Major settlement may take place due to the accumulation of slight plastic deformity due to single wheel loads. Stabilization of subgrade should be identified for both static and cyclic loading.

Unstable subgrade contains fine soil particles, which have low stability and low permeability than coarse soil particles. Generally, soil with fine particles and/or high plasticity soil can exist in zones that have low performance. Grain size distribution of subgrade is not uniform in ballast or subballast layer along the wheel length. The most prevalent type of soil that is used for subgrade is fine soil particles, while the use of coarse soil particles for subgrade is rare.

As coarse-grained soil types are insignificantly influenced by the subgrade water content, fine-grained soils are highly vulnerable to environmental factors. With increasing subgrade water content, strength and stiffness of fine-grained soil are significantly reduced, resulting in higher plastic deformation under cyclic train loads, consolidation settlement or massive shear failures. Moisture content of the soil has a deep impact on subgrade performance.

Soil suction is considered a main factor that can restrain the effective shear stresses of soil. Matricsuction depends on the grain size distribution, type of soil, ratio of fine particles . . .etc. (Bishop & Blight, 1963).

Progressive shear failure and excessive plastic settlement are the primary failure modes of rail track subgrade (Selig & Waters, 1994). The first type of failure is caused by overstresses on the subgrade due to cyclic loads. Soil of subgrade progressively squeezes out beneath tie and then moves upward at the end of tie following the direction of low resistance. Subgrade is progressively sheared and reformed due to cyclic overstresses and then leads to subgrade shear failure (Li & Selig, 1996). Due to repetition of overstresses, surface soil migrates in an up and side direction and follows the way of low resistance (Li *et al.*, 2016).

When the subgrade is constructed as part of an embankment, the stress on the foundation of the embankment will be in excess as a result of the additional weight from the embankment. Massive shear failure will occur due to pore water pressure if the embankment is not drained. Dissipation of pore water pressure and settlement are analyzed in basic consolidation theory. Rapid settlement could happen in coarse soil due to rapid dissipation of excess pore pressure, and this may happen at the time of embankment construction. While in fine soil, the settlement occurs after construction because of the slowly dissipation of pore pressure.

The volume change varies along the track and may lead to settlement (shrink) in some locations and heave (swell) in others, affecting track geometry. The largest volume change typically occurs on the initial swell of partially saturated soils. While the slope corrosion happens due to surface or subsurface water flowing. Occasionally, the wind also causes corrosion of subgrade slopes or toe surface erosion that may not immediately affect track

operation. But if this surface erosion is not repaired, the increase in erosion can cause an undermined track, sinkholes and sometimes effects on track stabilization.

Track subgrade may be more subjected to progressive shear failure even if the stress is less than its monotonic strength (Loh & Nikraz, 2012). In 2011, Burrow discussed that periodical loading could increase the plastic deformity over the threshold stress and decrease to a steady state below the threshold stress. There are several factors that affect excessive plastic deformation, such as vertical strain of progressive shear deformation, deformation due to gradual compaction, type of soil, consolidation of whole rail track subgrade and soil water characteristics (Leshchinsky & Ling, 2013). Water collected within these ballast pockets can further weaken the subgrade, introducing mud-pumping (Burrow *et al.*, 2011).

In order to avoid at least two main failure types, especially in the top layer where the stress is critical, these three factors should be considered during the design of track foundations (Burrow, Bowness, & Ghataora, 2007). Percentage of fine particles and water content of subgrade is considered two internal factors that govern the track foundation failure, while cyclic loads are considered an external factor which is used in laboratory experiments to represent train traffic loads.

There are three types of loading that affect the foundation of a track, which include static, cyclic (periodical) and dynamic. To design and remediate a rail track foundation, the quantification of the load environment is important (Li *et al.*, 2016). Combined effects of live loads from train weight and dead load weight of the rail structure are known as a static load on a rail track foundation. Effects of dead loads are hidden in track foundation design guidelines; however, live load is dominant. A conventional guideline is based on the actual axle load in foundation designs (Burrow, Ghataora, & Evdorides, 2011; Dareeju, 2017; Li, Chen, Zou, & Chen, 2023; Feng, Luo, Wang, Connolly, & Liu, 2024).

The change in soil shear strength can be caused by repeated loading depending on the soil's physical properties (degree of saturation and void ratio). A stress smaller than the static failure stress, when applied repeatedly, can cause very large strain that will be defined as a failure condition (Lambe & Whitman, 1969). However, below the level of static strength of soil, there exists a maximum stress level below which deformation becomes stabilized. Previous studies of the cyclic behavior of unsaturated soil concentrate on three aspects: resilient modulus, accumulation of plastic strain and liquefaction potential. The first two aspects are closely related to railway subgrade and pavement design. The third aspect is more relevant to earthquake engineering.

Loh and Nikraz (2012) investigated the behavior of kaolinite clay as fine-particle soil using undrained triaxial testing. Also, the properties of subgrade response that developed due to traffic of wheel loading of modern train speed were simulated. Four types of both cyclic and static undrained triaxial tests were performed. The results explained that there is a threshold for the clay subjected to high repeated loads when the effective shear analysis was used. Additionally, the study proposed a new approach that rationalized and reformulated the current state of the design and management process of railway track substructures involved clay subgrade.

Hayano, Ishii, and Muramoto (2013) studied the characteristics of ballast settlement due to the effect of ballast thickness and tie-tamper repair. A set of experiments using cyclic loading tests on model ground was performed. Results suggested that the 250 mm ballast thickness currently adopted as the standard design is ineffective for minimizing settlement that occurs when the nonlinearity of roadbed compressibility is relatively moderate. Moreover, characteristics of the initial settlement process are altered significantly after tie-tamper implementation, although the degree of gradual subsidence undergoes minimal change regardless of ballast thickness and roadbed type.

Sivakumar *et al.* (2013) investigated the behavior of unsaturated soil with an effect of cyclic loads. As part of the research, a triaxial system was developed that incorporates small-

strain measurements using Hall effect transducers, in addition to suction measurements taken using a psychrometer. A condition of constant water content was adopted to apply the experiments to a sample of kaolin. They concluded that when the number of loading cycles was increased, the suction of the sample was reduced. Also, the resilient modulus initially increased with increasing water content up to approximately optimum water content and then reduced substantially with further increase in water content.

A half-full-scale railway was constructed by Fattah, Mahmood, and Aswad (2019, 2024) for carrying out the tests. Three ballast thicknesses of 200, 300 and 400 mm were used in the tests. The ballast was overlying 500 mm thickness clay in two states, soft and stiff. The tests were carried out with and without geogrid reinforcement. Settlement in ballast and clay, soil pressure and pore water pressure induced in the clay were measured in reinforced and unreinforced ballast cases. It was concluded that the amount of settlement increased as the simulated train load amplitude increased, and there was a sharp increase in settlement up to cycle 500. After that, there was a gradual increase that leveled out between, 2,500 and 4,500 cycles, depending on the frequency used. There was a slight increase in the induced settlement when the load amplitude increased from 0.5 to 1 ton, but it was higher when the load amplitude increased to 2 tons.

Experiments were carried out by Fattah, Majeed, and Joni (2024) using models that simulate a railway with nearly half the scale of the real one. The tests were carried out using different load amplitudes and frequencies. These experiments investigated the effect of the subgrade degree of saturation on the value of the stresses generated on the surface and the middle (vertical and lateral stresses) and the settlement of the subgrade. The results of the investigation demonstrated that, while load frequency had a minimal effect on track-panel settlement, it increased with the load amplitude and subgrade soil saturation degree. The change of settlement of the track panel with the number of cycles has a high rate at the beginning; after a while from that, it decreases gradually until, after some value of the number of cycles, the settlement changes at a very low rate and gradually.

The present paper investigates the influence of the railway track cyclic load on the behavior of saturated and unsaturated subgrade clayey soil layers. According to that, the objectives of this study can be identified by studying the effect of subgrade layer degree of saturation variation, load amplitude and load frequency on the transmitted stresses through the ballast layer to the subgrade layer and the stress distribution inside it, and investigating the excess pore water pressure development in the clay layer in the case of a fully saturated subgrade layer and the change in matric suction in the case of an unsaturated subgrade layer. In addition, investigations of the effect of subgrade layer degree of saturation variation, load amplitude and load frequency on the track panel and subgrade settlement have been made.

2. Laboratory work and material properties

The laboratory models that are used in the present tests are almost half scale of the actual scale of the rail truck that is in the Iraqi railway service. The experimental program of the tests includes a number of laboratory models performed to investigate the stress and settlement of unsaturated soil (subgrade) under railway cyclic loading. This was performed by testing a series of models that have different subgrade layer saturation degrees (Sr.%) using different values of load frequency and load amplitude.

2.1 Materials used

2.1.1 The soil. In this research, clayey soil of brown color was used. The soil was brought from an old embankment around Baghdad city. Standard tests were performed to determine the

physical properties of the soil. The details of the soil characteristics are listed in Table 1. The soil is classified as (CL) according to the Unified Soil Classification System.

2.1.2 Ballast. The main physical properties of the used ballast are illustrated in Table 2. According to the Unified Soil Classification System, the ballast can be classified as (GP) poorly graded ballast.

2.1.3 Geogrid reinforcement. The used geogrid in the experimental tests is tensar type SS2, as shown in Plate 1. This type of geogrid used for reinforcement of soil and aggregate is produced by Tensar International; its engineering properties are shown in Table 3 as provided by the manufacturing company. The sheet of geogrid was used in multiple tests but was replaced whenever it became visibly overstressed or damaged. The selected geotextile must meet the following four durability criteria.

(1) It must be tough to withstand the stresses during the installation process. Properties concerned are:

- (1) Tensile strength. (2) Burst strength. (3) Grab strength. (4) Tear strength. (5) Resistance to ultraviolet (UV) light degradation for two weeks exposure with negligible strength loss.

(2) It must be strong enough to withstand static and dynamic loads, high pore pressures and severe abrasive action to which it is subjected during its life-span. The properties concerned are:

Test	Magnitude	Specification
Classification (USCS)	CL	ASTM D 2487 (2017)
Activity	0.41	–
Clay %, <0.005 mm	42	ASTM D 422 (2007)
Silt %, 0.005–0.075 mm	28	ASTM D 422 (2007)
Sand %, 0.075–4.75 mm	30	ASTM D 422 (2007)
Gravel %, >4.75 mm	0	ASTM D 422 (2007)
Specific gravity (Gs)	2.7	ASTM D 854 (2023)
Liquid limit (LL)	33	ASTM D 4318 (2017)
Plastic limit (PL)	18	ASTM D 4318 (2017)
Plasticity index (PI)	15	ASTM D 4318 (2017)

Note(s): * Activity = (PI/{percent of clay <0.002 mm})
Source(s): Authors' own work

Table 1. The used clay physical characteristics

Property	Magnitude
Minimum dry unit weight $\gamma_{dry\ min}$, kN/m^3	15.43
Maximum dry unit weight $\gamma_{dry\ max}$, kN/m^3	19.17
Used dry unit weight $\gamma_{dry\ used}$, kN/m^3	18.21
Relative density, R.D, %	78
D_{60} mm	22.6
D_{30} mm	20.4
D_{10} mm	17.5
Coefficient of uniformity, C_u	1.29
Coefficient of curvature, C_c	1.05

Source(s): Authors' own work

Table 2. The properties of used ballast

Source(s): Authors' own work

Plate 1.
Geogrid reinforcement used in tests

Property	Units	
Polymer (1)		PP
Minimum carbon black (2)	%	2
Roll width	m	4.0
Roll length	m	50
Unit weight	Kg/m^2	0.29
Roll weight	Kg	60
Dimensions		
A_L	mm	28
A_T	mm	40
W_{LR}	mm	3.0
W_{TR}	mm	3.0
t_J	mm	3.8
t_{LR}	mm	1.2
t_{TR}	mm	0.9
Rib shape	Rectangular	
Quality control strength (longitudinal)		
T_{ult} (3)	kN/m	17.5
Load at 2% strain (3)	kN/m	7.0
Load at 5% strain (3)	kN/m	14.0
Approximate. strain at T_{ult}	%	12.0
Quality control strength (transverse)		
T_{ult} (3)	kN/m	31.5
Load at 2% strain (3)	kN/m	12.0
Load at 5% strain (3)	kN/m	23.0
Approximate. strain at T_{ult}	%	10.0
Junction strength as % of QC strength (4)		
Minimum junction strength	%	90

Note(s): (1) PP denotes polypropylene
Source(s): Tensar International (2011)

Table 3.
Tensar SS2 geogrid specification

- (1) Puncture resistance. (2) Abrasion resistance. (3) Elongation at failure.

(3) It must be resistant to excessive clogging or blinding, allowing water to pass freely across and within the plane of the geotextile. At the same time, it must be capable of filtering out and retaining fines in the subgrade. The properties concerned are:

- Cross-plane permeability or permittivity
- In-plane permeability or transmissivity
- Apparent opening size (AOS).

(4) It must be resistant to rot and attacks by insects and rodents. It must be resistant to chemicals, such as acids and alkalis and to the spillage of diesel fuel.

2.2 Soil suction measurement

The metric potential sensor represents indirect methods to measure the soil matric suction by using a pair of discs of porous ceramic consisting of a fixed matrix. To shape a capacitor, the pair of discs are isolated from each other by a printed circuit board. The water content of the ceramic disc will alter in case the sensor becomes in touch with soil.

With the passage of time, the fixed-matrix ceramic disc suction and the soil suction will be in equilibrium; when that happens the soil and the ceramic disc should have the same suction magnitude. The water content of the ceramic disc will be measured by the sensor, and that value of water content will be converted to suction magnitude according to the relation of the fixed-matrix ceramic discs water content with its suction value that was previously determined.

Under specific conditions in a period of a few hours, the sensor, which can measure a varying high magnitude of suction (almost 10,000 kPa or higher) (Tripathy, Al-Khyat, Cleall, Baille, & Schanz, 2016). The disc is 32 mm in diameter and the assembly part about 35 mm.

2.3 Models tests

A special apparatus system was used in performing the experimental laboratory testing work, which produced different capacities of dynamic (cyclic) loads and frequencies and was designed and manufactured. A number of accessories were made in order to simulate the actual loading condition of railway track as much as possible to actual railway track loading in the field. The testing apparatus system was utilized to study the stress–strain response of unsaturated soil of subgrade under the railway track loading to achieve the aims of this study.

The testing apparatus system components are: loading frame made of steel, two hydraulic loading systems, steel beam of dimensions (800 mm × 65 mm ×65 mm) as load distributor, two data acquisition systems, shaft encoder and container of dimensions (1.5 m length × 1 m width × 1 m height).

The hydraulic loading system produces a maximum load frequency of 2 Hz. A new modification was made to increase the frequency up to 4 Hz. The apparatus system used in performing the testing is shown in Figure 1.

The traffic loading simulation on the sleepers was executed by applying rectified sine wave loading. This type of loading was suggested by Awoleye (1993). It simulates a running of train over three sleepers in which 50% of the wheel load is transmitted to the middle sleeper and 25% of the wheel load on both outer sleepers.

In order to exert the load on the track panel in a proper and correct way, a solid steel beam was utilized that has dimensions of (800 mm × 65 mm ×65 mm) as depicted in Plate 2. A steel container of dimensions (1.5 m length ×1 m width ×1 m height), made of steel plate

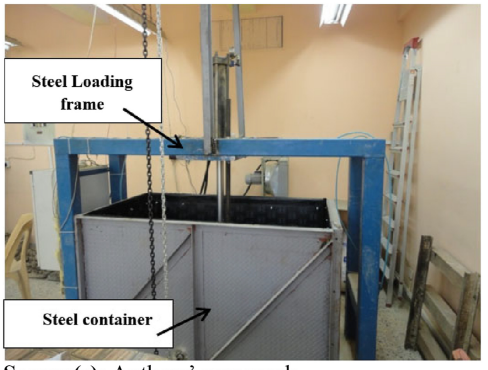

Source(s): Authors' own work

Figure 1.
The used apparatus loading system

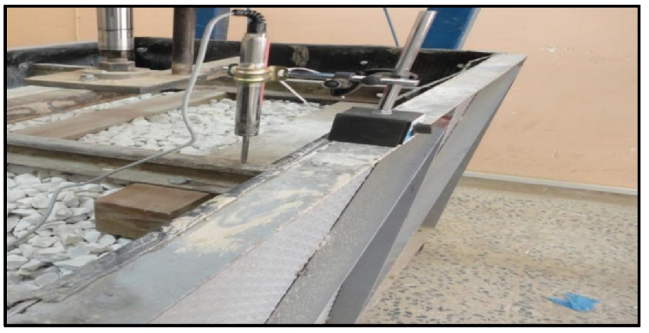

Source(s): Authors' own work

Plate 2.
Load distributor beam

5 mm thick well-welded parts, was used to perform the tests of the half-scale model. An external bracing was made by angles at edges on the long sides, as was the base that has been strengthened by three external channels (50 mm web × 25 mm flange).

Two data acquisition systems were utilized; the first one was used to evaluate and record the displacement of the main hydraulic cylinder jack shaft when implementing the test, which enabled the tester to obtain large and accurate data of displacement in a very short time. The data acquisition was also used to select the required frequency of the test, which comes up to 4 Hz.

Three pressure cells were used in the laboratory models, they are heavy duty cells of Model 3515 Geokon, which is suitable for railroad ballast pressures measurement and two heavy duty cells of Model 3500 Geokon that are used to measure the pressure in clay layers (subgrade).

A Geokon Model 3400 Series heavy-duty Piezometers were used to measure pore-water in fully saturated models; these piezometers are used for dynamic pore-water pressures measurements in concrete structures, bore holes, wells, pipe lines, embankments, etc.

The track panel that is used in the laboratory models is composed of a pair of rails 800 mm in length and three sleepers made from wood of dimensions (900 mm × 100 mm x 100 mm) as shown in Plate 2. The center-to-center spacing for the rails is 650 mm, while for the sleepers it was 300 mm. The utilized rail in this work has a dimension that represent almost half scale of the real rail dimensions of 60 kg (UIC) type (Chandra & Agarwal, 2007).

2.4 Model preparation

Laboratory models of half-scale railway were used to carry out the experimental tests. The tests were performed in a well-tied box made from steel of dimensions (1,500 mm length × 1,000 mm width ×1,000 mm height). In order to reduce reflection of waves through the test; the test box was cushioned utilizing a pair of layers, the first one comprises of packed styropor sheets 5 mm thick, while the second one is rubber 4 mm thick. Each model consists of a 500 mm clay layer, a 200 mm ballast layer overlying the clay layer and finally, a track panel composed of a pair of rails 800 mm in length and three sleepers made from wood of dimensions (900 mm × 100 mm x 100 mm). The track panel is placed on the top of the ballast layer. Figure 2 shows the laboratory test section.

In order to perpetrate a homogeneous clay layer, a number of tests and measurements were conducted to check that the method of preparation gives a homogenous clay soil layer. In order to ensure that the compaction energy reaches all the clay within the layer, it was decided to construct small layers similar to the procedure followed in the standard compaction test. Portable vane shear (ASTM D 4648, 2005) and unconfined compression tests were performed. Eight samples with different water contents to get different degrees of saturation (100, 80, 70, 65, 60, 55, 50 and 40%) were prepared and stored in sealed plastic bags for 72 hours in order to achieve uniform distribution of water as recommended by Tripathy *et al.* (2016). The samples were prepared at a dry unit weight of 16 kN/m^3 using modified Proctor mold tamped gently with a special compaction hammer. A thick sheet of plastic were utilized to cover the test specimens. The specimens were tested every day for a seven-day period. The aim of this test is determining the change in the undrained shear strength of the remolded soil with time to regain its strength after the mixing process. The relation of undrained shear strength with degree of saturation Sr. % from the unconfined compression test and vane shear test after seven-day molding is shown in Figure 3.

The test was carried out at the room temperature, which ranged between (23 and 26)ºC since the soil suction is affected by changes in temperature.

The results showed that the soil regains its strength within two days in cases of 100 and 80% degree of saturation and four days in cases of 70 and 60 % degree of saturation. The value of Cu obtained from the vane shear test is less than the unconfined compression test, especially for a degree of saturation less than 70 % with Cu greater than 50 kN/m^2, which are defined as hard (Mayne, Christopher, & DeJong, 2001). This behavior may be imputed to mean that these samples may deviate from the presupposed cylindrical failure surface, resulting in an error in the measured strength (ASTM D 4648, 2005).

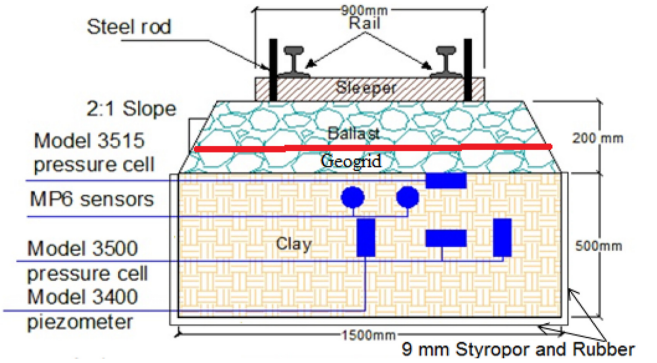

Figure 2.
Section through the laboratory model

Source(s): Authors' own work

At first, the soil sample for many days was air-dried and crunched till it became as fit as to pass through a #10 sieve (the sieve opening size is 2 mm). The initial water content of the crunched soil after that was measured according to (ASTM D 2216, 2019).

The soil was mixed with water by a large mixer at 25 kg per one mixing portion of soil for adequate time to be homogenous. The soil was stored in plastic bags of 50 kg capacity for a period of seven days or more to achieve a regular water distribution. After that, the soil was compacted by using a special compaction device to the required dry unit weight (16 kN/m^3). The soil was constructed in 500 mm depth, the compaction was done in seven layers, six of them were 70 mm thick and one was 80 mm thick.

At a depth of 250 mm from the soil surface (at the middle of the layer), two pressure cells Model 3500 were instilled under the rail at the middle sleeper. One of these pressure cells was laid horizontally to measure the vertical stresses and the second one was laid vertically to measure the lateral stress.

The second stage in model preparation was the ballast layer construction. A ballast layer of 200 mm thickness was placed at the top of the clay layer, which was prepared previously.

After the storage period of the clay layer was completed (from five to seven days), the soil suction of the soil in case of unsaturated soil should be measured and the reading of the suction value is compared with the SWCC to evaluate the degree of saturation of the clay soil layer. The undrained shear strength and water content of the clay layer should also be measured.

The ballast was constructed guardedly in three layers; each layer is about 65 to 68 mm thick until reaching the required thickness (200 mm). Each layer was compacted carefully by a tamping rod to get a dry unit weight of about 18.21 kN/m^3 and a relative density of about 78%. This was done by implementing a layer of ballast with a predetermined volume and weight. Inside the ballast layer, the geogrid was placed in a prearranged location at a depth of (1/2) of ballast thickness (100 mm from the surface of ballast), according to Fattah, Al-Mosawi, and Al-Ameri (2017). The ballast side was sloped down on about 2:1.

The final stage of model preparation is track panel placement. Before track panel placement, the ballast top surface should be leveled as much as possible to get good seating track panel on the surface of the ballast. After placing the track panels in its proper position, it was tamped carefully by using a bubble level to obtain a good track panel leveling. In order to achieve a panel track accurate restriction, an additional ballast quantity should be added around the panel track and at the spaces between the sleepers.

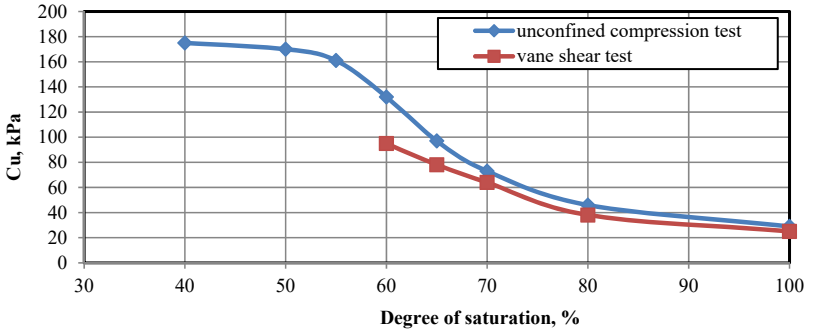

Source(s): Authors' own work

Figure 3. Variation of the undrained shear strength Cu with degree of saturation Sr.% from the vane shear and unconfined compression tests

3. Results and discussion

3.1 Soil pressure

The effect of subgrade layer degree of saturation on the pressure distribution and magnitude is presented in Figures 4–11. Figures 4 and 5 show the values of the average maximum vertical pressures; these were measured by a pressure cell placed on the surface of the subgrade layer that was named in this work as (Surface). These figures are drawn for 15 and 25 kN load amplitudes. The results clearly indicate that pressure at the surface of the subgrade layer increases with the degree of saturation decreasing. Furthermore, the data show that the increase of pressure when the Sr. is reduced from 100 to 80% has a lower value than cases when the Sr. is reduced from 80 to 70% or from 70 to 60 %.

It should be noted that the lower subgrade layer degree of saturation means stiffer soil due to increasing matric suction and increase in effective stress and thus shear strength. In other words, the stiffer subgrade will receive higher values of pressure transferred from the upper ballast layer. This behavior of pressure at the subgrade layer surface is a result of stress concentration under sleeper load position; it means that in the soil of higher stiffness, the stresses will be concentrated under the position of load application in a higher value from those soils with less stiffness value.

Also, the stiffer soil has more capacity to carry higher pressure than the soft one with less generated settlement. That will lead to higher generated stresses in the stiffer soil than softer soil according to the higher resistance that the stiff soil will show to the settlement. This finding agrees with the result and conclusion of Fattah, Mahmood, and Aswad (2022), who noted that for unreinforced and reinforced ballast, measurements of the pressure cell at the surface of the subgrade layer and the piezometer measurements have a higher value at stiff clay than the soft one.

It can be noted that for deep pressure values, the decrease of Sr. results in increases in deep pressure values. The increasing in pressure was moderated when the Sr. changed from 100 to 80%, except under load amplitude 35 kN and load frequency 2 and 4 Hz. For example, at load amplitude 35 kN and frequency 2 Hz, the pressure increased from 22.8 to 34.5 kPa when the Sr. was reduced from 100 to 80%, this means about a 50% increase in pressure. In case of Sr. reduced from 80 to 70 and down to 60 %, the pressure increased from 34.5 to 53.3 and 73.1 kPa, which is about 54 and 37%, respectively. At load amplitude 15 kN and frequency 2 Hz as in Figure 8, the pressure increased from 12.04 to 14.88 kPa when the Sr. was reduced from 100 to 80%, which represents about 23.5 % increase in pressure. In case of Sr. reduced

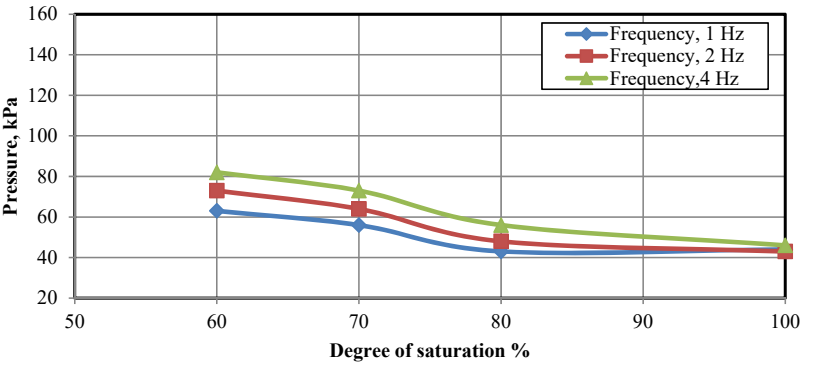

Figure 4.
Relation between the degree of saturation and pressure in the surface cell under 15 kN load amplitude

Source(s): Authors' own work

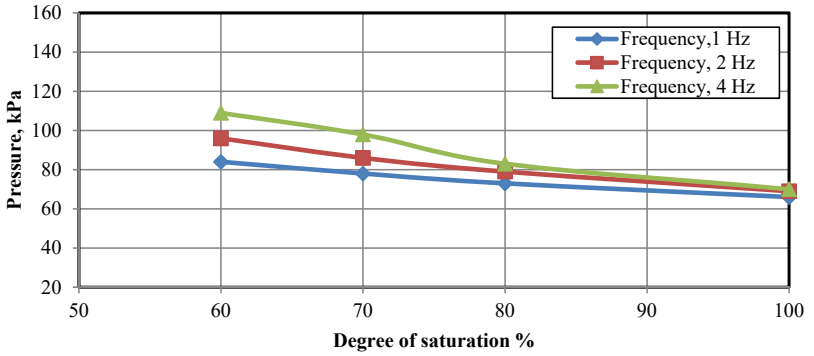

Source(s): Authors' own work

Figure 5. Relation between the degree of saturation and pressure in the surface cell under 25 kN load amplitude

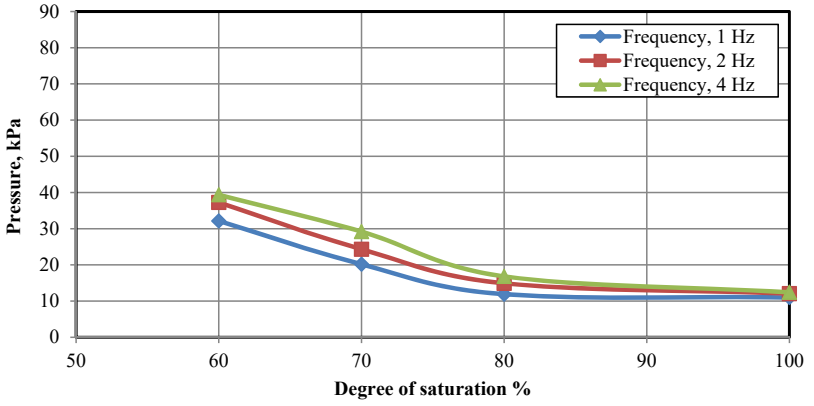

Source(s): Authors' own work

Figure 6. Relation between the degree of saturation and pressure in the deep cell under 15 kN load amplitude

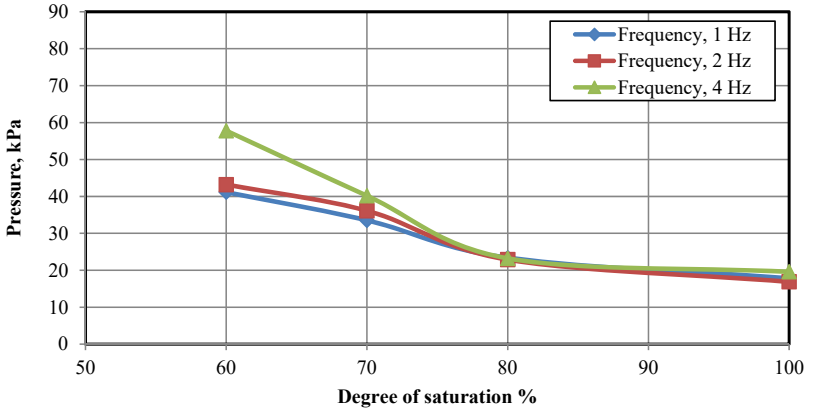

Source(s): Authors' own work

Figure 7. Relation between degree of the saturation and pressure in the deep cell under 25 kN load amplitude

from 80 to 70 and down to 60 %, the pressure increased from 14.88 to 24.32 and 37.23 kPa, which represents an increase about 63 and 53 %, respectively.

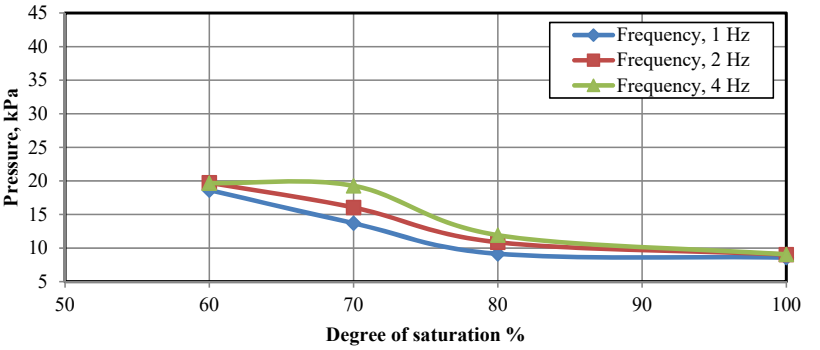

Figure 8.
Relation between the degree of saturation and pressure in the lateral cell under 15 kN load amplitude

Source(s): Authors' own work

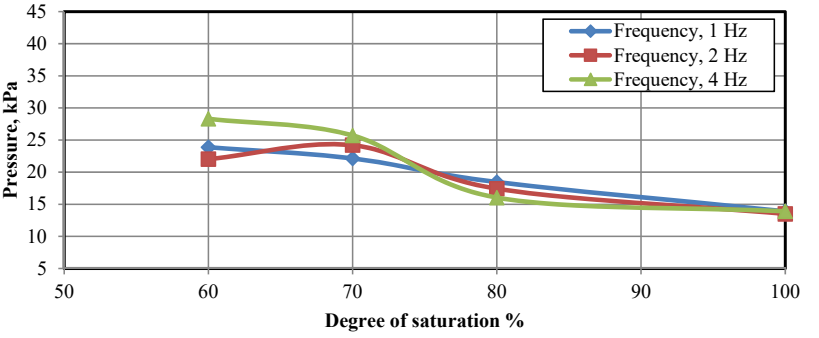

Figure 9.
Relation between the degree of saturation and pressure in the lateral cell under 25 kN load amplitude

Source(s): Authors' own work

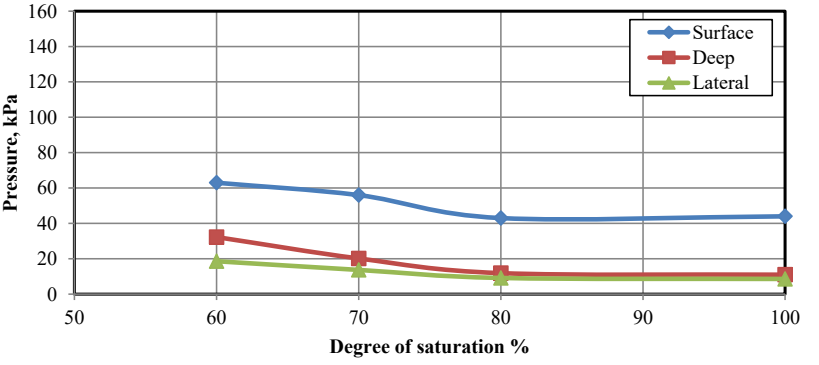

Figure 10.
Relation between the degree of saturation and pressure for frequency 1 Hz under 15 kN load amplitude

Source(s): Authors' own work

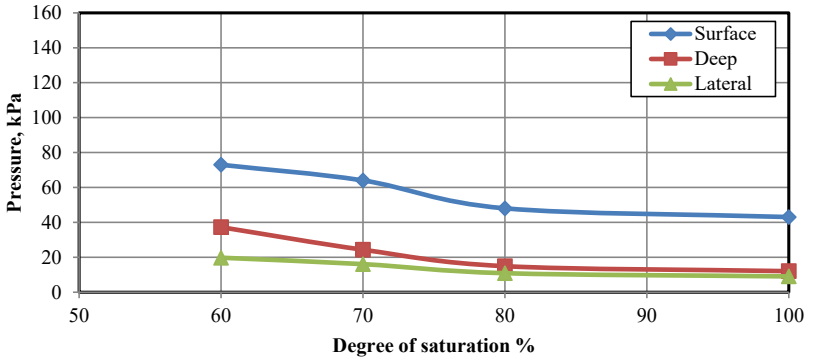

Source(s): Authors' own work

Figure 11. Relation between the degree of saturation and pressure for frequency 2 Hz under 15 kN load amplitude

It should be noted that in the case of load 15 kN and frequency 2 Hz, if the pressure value at Sr. 100% is considered as a reference, the increase in pressure value when the saturation value is reduced from 100 to 80 and then to 70 down to 60%, the increase rate is 23, 101 and 209 %, respectively. The same observation about the load amplitude of 15 kN can be seen in other load values; 25 and 35 kN.

Figures 8 and 9 present the relationship between the degree of saturation of the subgrade layer and the average maximum lateral pressures. The lateral pressure was measured by the installation of a pressure cell in a vertically lateral position at the middle of the subgrade layer next to the deep pressure cell. The results clearly indicate that with the subgrade layer Sr. decreasing, the value of lateral pressure increased. It can be noted in Figure 10 that for load amplitude 15 kN, the pressure revealed a higher increasing rate after Sr. 80%. Furthermore, the data in the figure show that for frequency 4 Hz, the increase in pressure is almost negligible when the Sr. is reduced from 70 to 60%.

In Figure 9, which is for load amplitude 25 kN, it can be noted that at the load frequency of 2 Hz, the pressure is decreased when the Sr. decreases from 70 to 60%. Indeed, this observation about the pressure value reduction with the Sr. reduction is only observed at load 25 kN and frequency 2 Hz. For load amplitude 35 kN, the results indicate that with Sr. increasing, the pressure value is increased and for all load frequency values that were used. It can also be noted that for load frequencies 2 and 4 Hz, the pressure values are very close to each other. The increase in lateral pressure has a lower rate when the Sr. decreased from 70 to 60% than when it was reduced from 80 to 70%. For example, for load 35 kN and frequency 2 Hz, when the Sr. decreased from 100 to 80 and reduced to 70 % down to 60 %, the lateral pressure increased from 17.78 to 26.26, 35.73 and 39.5 kPa, respectively.

It can be also noted that for load frequency 4 Hz, the change of Sr. from 70 to 60% has shallow influence on the pressure value.

Figures 10 and 11 present a comparison of pressure values measured by the surface, deep and lateral pressure cells with the change in degree of saturation of the subgrade layer. These figures are drawn for a single value of load amplitude and frequency. The values of pressure for the lateral and deep cells are advanced parallel when the Sr. is reduced from 100 to 80% but after Sr. reduction from 80 to 70, reaching 60%. It can be noted that the rate of pressure increasing is higher at deep pressure cells, which is confirmed by Figures 10 and 11.

3.2 Pore water pressure in saturated subgrade layer

Figures 12–17 show the relation between the number of cycles and the generated pore water pressure for fully saturated soil of the half-scale laboratory model. Figures 12 and 13 are

drawn for load amplitudes 15 and 25 kN, respectively, at load frequency 1 Hz. These figures show that the built up of excess pore water pressure reached its maximum value

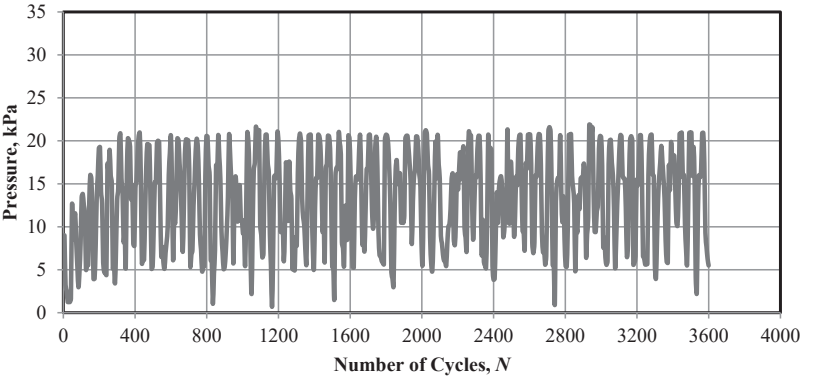

Source(s): Authors' own work

Figure 12.
Pore water pressure development with number of cycles under load amplitude 15 kN, frequency 1 Hz

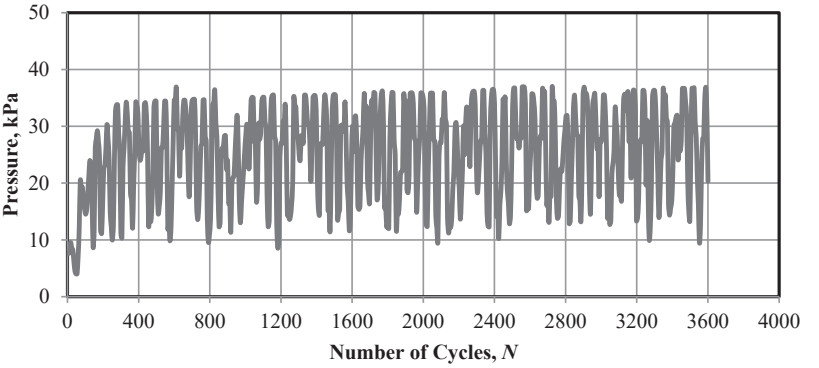

Source(s): Authors' own work

Figure 13.
Pore water pressure development with number of cycles under load amplitude 25 kN, frequency 1 Hz

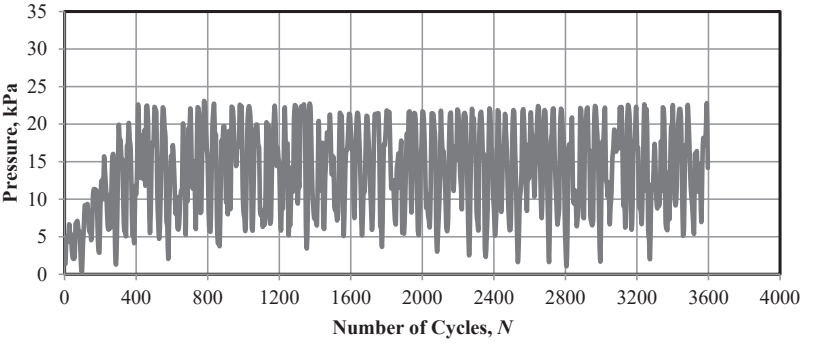

Source(s): Authors' own work

Figure 14.
Pore water pressure development with number of cycles under load amplitude 15 kN, frequency 2 Hz

approximately at 250 cycles when the load frequency is 1 Hz and about 400 and 650 cycles when the load frequencies are 2 and 4 Hz, respectively.

It can also be observed that the initial value is about 45 % from the maximum pore pressure value for the load frequency of 1 Hz. The initial value of pore water pressure is about 30% from its maximum value for load frequency 2 Hz and about 25 % for the load frequency

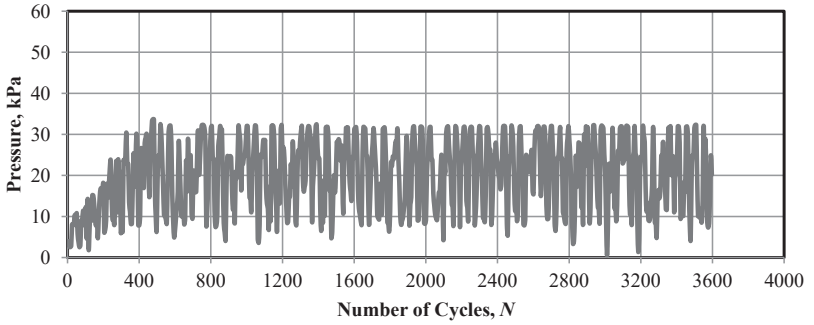

Source(s): Authors' own work

Figure 15. Pore water pressure development with number of cycles under load amplitude 25 kN, frequency 2 Hz

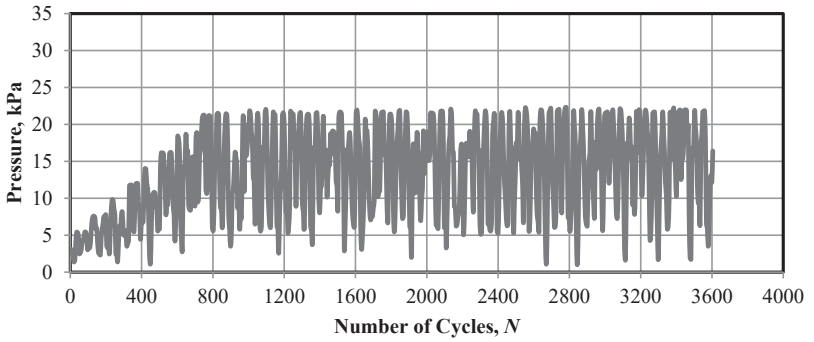

Source(s): Authors' own work

Figure 16. Pore water pressure development with number of cycles under load amplitude 15 kN, frequency 4 Hz

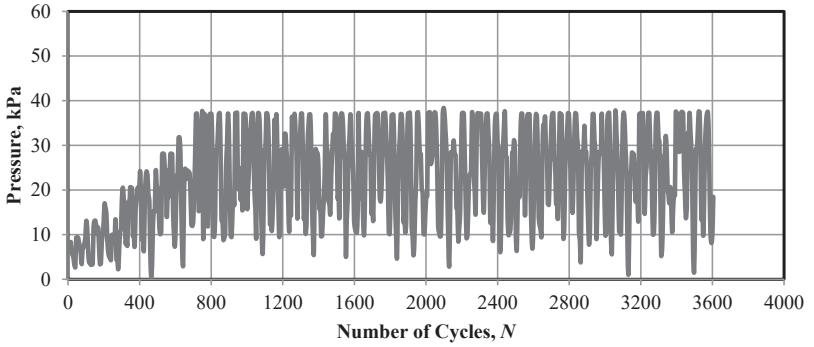

Source(s): Authors' own work

Figure 17. Pore water pressure development with number of cycles under load amplitude 25 kN, frequency 4 Hz

4 Hz. The above observation is almost the same for load amplitudes 25 and 35 kN, as shown in Figures 14–17.

Indeed, the time built up for load amplitudes 15, 25 and 35 kN is about 250 s to reach its maximum value for load frequency 1 Hz. While in the case of load frequency 2 Hz, it is approximately 200 s for load amplitudes 15, 25 and 35 kN, in the case of load frequency 4 Hz, the time of pore pressure built up for load amplitudes 15, 25 and 35 kN is about 160 s.

It can be concluded from the above behavior that for all load amplitudes used in laboratory models (15, 25 and 35 kN) and load frequency that:

(1) For higher values of the load frequency, it took more cycles but less time to reach its maximum value.

(2) The initial value of pore water pressure as a percent from the maximum value of pore water pressure is higher when the load frequency is lower. This finding agrees with Li and Selig (1996), Wichtmann, Andersen, Sjursen, and Berre (2013) and Fattah *et al.* (2017), who stated that in general, at lower frequencies and for a given number of cycles, larger pore pressures were generated.

(3) There is no effect of load amplitude either on time or number of cycles for pore pressure built up. Loh and Nikraz (2012) found that it seems carrying on of loading implementation at higher loading frequency, in any case, creates a similar measure of excess pore pressure develop build-up and total strain accumulation like that for lower loading frequency, at the higher number of loading cycles.

(4) There is no effect of load amplitude on the initial pore pressure value as a percent of the maximum pore pressure value.

It can be noticed that the measured excess pore water pressure increases with operating frequency, reaching a steady state value at a frequency of about 4 Hz for all models. The figures illustrate that the operating frequency in the range of 1–4 Hz is the most effective in buildup of pore water pressure. The rate of increasing the pore water pressure possesses its maximum value at the resonance frequency; after that, the rate is reduced remarkably (Fattah *et al.*, 2017).

3.3 The reduction of matric suction in unsaturated subgrade layer

In order to determine the reduction in matric suction of unsaturated half-scale laboratory models, the initial values of suction were recorded immediately before performing the loading test.

The matric suction was measured at the middle of the subgrade clay layer (at adepth of 250 mm from the top surface of subgrade clay layer) beneath the cross point of rail and sleeper at middle sleeper. The final value of matric suction was measured again at the end of each test, the difference between the initial and final matric suction values represent the reduction in matric suction.

Figures 18 and 19 demonstrate the effect of load frequency at different initial degrees of saturation of the tests on the reduction of matric suction at the end of tests. The figures are for loads 15 and 25 kN at frequencies 1, 2 and 4 Hz. The results show that the increase in load frequency from 1 to 4 Hz has no effect on the value of reduction of matric suction for all tests with applied loads (15, 25, and 35 kN).

It can be seen that the value of reduction in matric suction of each load test amplitude of different frequency has almost the same value, the curves of frequencies 1, 2 and 4 and load amplitude 15 kN are almost lying on each other. That above observation of the load frequency effect is also noted for load amplitudes 25 and 35 kN. The load frequency effect is the same for the various values of degree of saturation as illustrated in Figures 18 and 19, which means

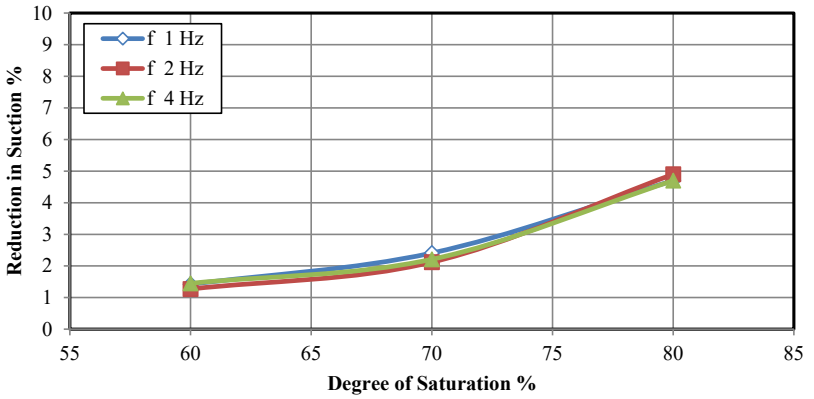

Source(s): Authors' own work

Figure 18. Relation between the reduction in suction with degree of saturation under 15 kN load amplitude

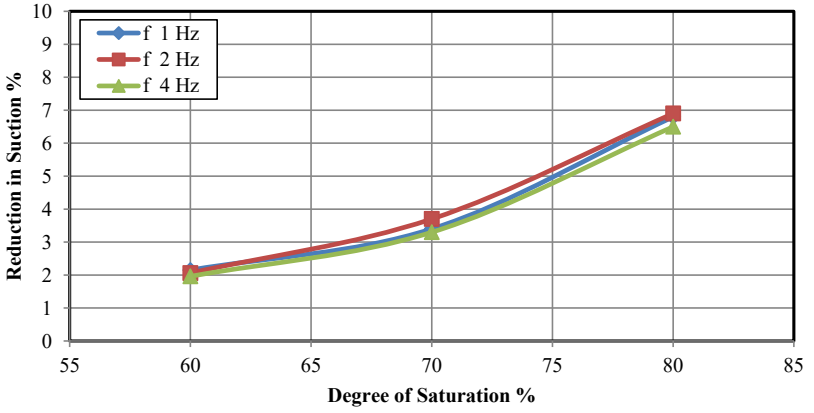

Source(s): Authors' own work

Figure 19. Relation between the reduction in suction with degree of saturation under 25 kN load amplitude

that the load frequency has no effect on the matric suction reduction for any load amplitude, and the frequency has no effect on the reduction of matric suction at any degree of saturation from 80 to 60%.

When soils are close to saturation, i.e. as Sr approaches unity, large changes in properties occur with small changes in suction. As soils become very dry, the changes in properties become considerably less (small values of Sr). In general, as the water content at compaction increases, the suction decreases.

It should be noted, however, that for the material in the railway track section, surcharge pressures reduce volume increases somewhat; the suction changes which might be measured during a wetting cycle with the type of apparatus available would be less than those which might occur in situ.

Figures 20–22 demonstrate the effect of load amplitude at different initial degrees of saturation of the tests on the reduction of matric suction at the end of these tests. Each figure is for a single value of load frequency and for three values of load amplitude. They reveal the relation between the degree of saturation and reduction of matric suction for load amplitudes

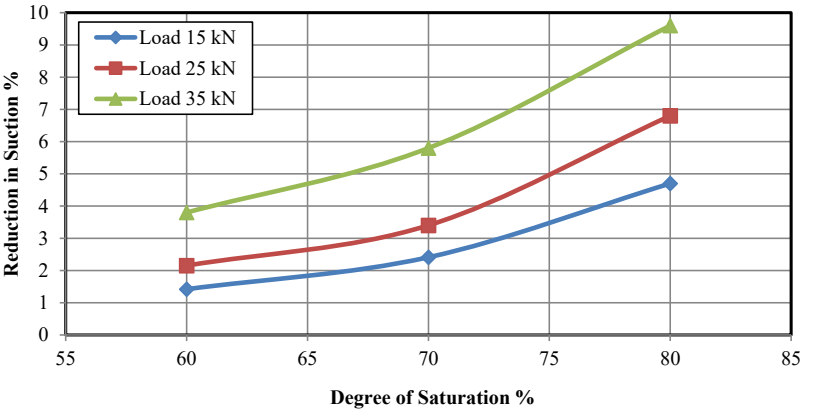

Figure 20.
Relation between the reduction in suction with degree of saturation of 1 Hz. frequency

Source(s): Authors' own work

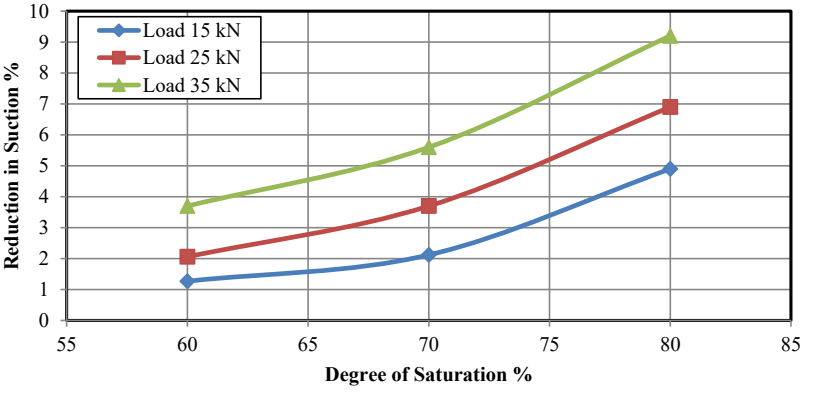

Figure 21.
Relation between the reduction in suction with degree of saturation of 2 Hz. frequency

Source(s): Authors' own work

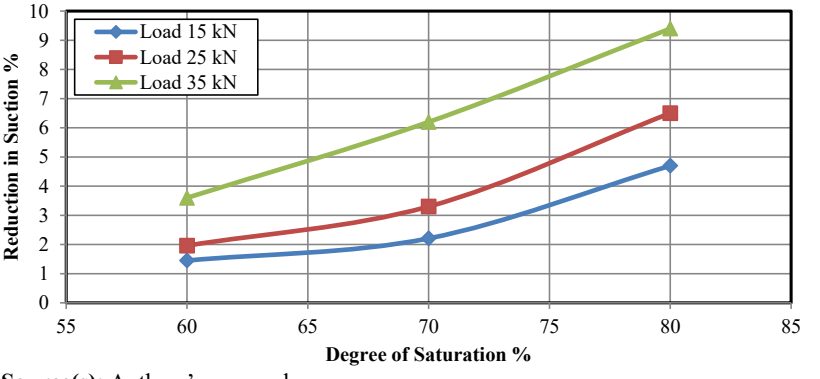

Figure 22.
Relation between the reduction in suction with degree of saturation of 4 Hz. frequency

Source(s): Authors' own work

15, 25 and 35 kN of load frequency 1 Hz. for Figure 20, 2 Hz. for Figures 21 and 4 Hz for Figure 22. These figures show that the reduction in matric suction increases when the load amplitude is higher; for example, at degree of saturation 60 % and load frequency 1 Hz, the reduction of matric suction is 1.42 and 2.15 % for load amplitudes 15 and 25 kN, respectively, and the reduction in matric suction is about 3.8 % for load amplitude 35 kN.

It can be noted that the value of matric suction reduction is higher with the higher load amplitude at all load frequencies 1, 2 and 4 Hz. and for all values of the degrees of saturation (60, 70 and 80 %) of tested models.

For all six figures of the matric suction changing, it can be noted that the percent of matric suction reduction is higher for higher degrees of saturation, as shown in the figures and for all load amplitudes and for all load frequencies, this means that the higher the water content, the more reduction in matric suction according to cyclic loading.

This observation about the degree of saturation and the reduction in matric suction under cyclic loading, which stated that the magnitude of the reduction was significant when the degree of saturation was high, agrees with the finding of Sivakumar *et al.* (2013), who concluded that variation of suction with the number of loading cycles during the repeated loading for the tests with an initial water content of value varying from 22 to 31%, subjected to different confining pressures. It was found that the initial suction reduced with compaction water content increasing, and repeated loading produces a further reduction in suction.

Also, it agrees with the result of Yang, Lin, Kung, and Huang (2008), who carried out a series of tests to examine the effects of matric suction on the resilient module of two different soils. The results showed a gradual reduction in suction with cyclic loading; the magnitude of the reduction was significant at a high degree of saturation (higher water content).

During the tests, there was a volume change (reduction in volume) according to load submitting, this reduction in volume led to a reduction in voids volume and precisely in volume of air in voids, this decreasing in volume of air leads to an increase in the degree of saturation of the soil. The soil with a higher degree of saturation has more tendencies to the volume change according to its low value of stiffness and shear resistance and therefore more reduction in voids volume.

This effect of reduction in matric suction will be higher for the soil of higher degree of saturation according to the fact that it has less matric suction value than the same soil of less degree of saturation, which makes it more sensitive for matric suction changing. For example, if the reduction in matric suction is 15 kPa for a soil that has initial matric suction 60 kPa, the percent of change will be 25 %, while for soil that has initial matric suction 1,000 kPa, the reduction was 150 kPa (ten times higher than the first soil), the percent of change will be 15 %.

It is not meaningful to evaluate the engineering properties of any soil unless its environment or soil moisture properties, are specified. For unsaturated soils, there is a considerable variation in properties corresponding to changes in soil moisture. Consequently, for the design of highways or railways, two sets of boundary conditions are required: material changes and significant changes in soil suction.

4. Conclusions

The most important conclusions that were deduced from the experimental laboratory half-scale models can be summarized as follows:

(1) The generated stresses of the subgrade layer soil.

- At load amplitude 15, 25 and 35 kN, the more load amplitude, the more stresses on the surface, deep and lateral pressure cells.

- The increase of load frequency has no or very small effect on the stresses at the surface, deep and lateral pressure cell at 100% subgrade layer saturation, but the lateral stress shows more response to the increase of frequency than deep and a surface pressure, while for Sr. 80, 70 and 60%, the higher load frequency results in a higher stress magnitude for the surface, deep and lateral, and that effect of the load frequency is higher when the Sr. is lower. Also, the increase in lateral stress value is higher when the frequency increased from 1 to 2 Hz than from 2 to 4 Hz for all Sr. % values of the subgrade layer.
- The lower degree of saturation results in higher stress values generated in the surface, deep and lateral pressure cell. The rate of stress increase according to Sr. % decreasing was higher at the surface pressure cell than deep pressure cell and lateral pressure cell. Also, this behavior was noted for deep and lateral comparison, in which the deep cell gives a higher increasing rate than lateral when the Sr. % of the subgrade layer is decreased.

(2) The generated pore water pressure in the subgrade layer as a result of cyclic loading at Sr. 100% was higher at lower load frequency of the same load amplitude. Also, the higher amplitude load generates higher pore water pressure but has no effect either on the time of occurrence or number of cycles for pore pressure built up. The initial value of pore water as a percent of the maximum value of the pore water pressure is higher for lower load frequency.

(3) The matric suction decreased with the advancement of the test (with the No. of cycles). The change in matric suction is higher for higher load amplitude. For the higher degree of saturation, the change of matric suction is higher than for the lower degree of saturation. There is no effect of the load frequency value on the change of the matric suction.

References

ASTM D 854 (2023). ASTM D 854, standard test method for specific gravity. American Society for Testing and Materials (ASTM).

ASTM D 2216 (2019). ASTM D 2216-98 standard test method for laboratory determination of water (moisture) content of soil and rock by mass. American Society for Testing and Materials (ASTM).

ASTM D 2487 (2017). ASTM D 2487-17, standard practice for classification of soils for engineering purposes (unified soil classification system). American Society for Testing and Materials (ASTM).

ASTM D 4318 (2017). ASTM D 4318, standard test method for liquid limit, plastic limit, and plasticity index of soil. American Society for Testing and Materials (ASTM).

ASTM D 422 (2007). ASTM D 422-00, standard test method for particle size analysis of soils. American Society for Testing and Materials (ASTM).

ASTM D 4648 (2005). ASTM D 4648-00, standard test method for laboratory miniature vane shear test for saturated fine-grained clayey soil. American Society for Testing and Materials (ASTM).

Awoleye, E. O. A. (1993). *Ballast type - ballast life predictions* (Vol. 122). Derby: British Rail Research LR CES. October 1993.

Bishop, A. W., & Blight, G. E. (1963). Some aspects of effective stress in saturated and unsaturated soils. *Geotechnique*, *13*(3), 177–197. doi: 10.1680/geot.1963.13.3.177.

Burrow, M. P. N., Bowness, D., & Ghataora, G. S. (2007). A comparison of railway track foundation design methods. Paper Presented at the Proceedings of the Institution of Mechanical Engineers. *Part F: Journal of Rail and Rapid Transit*, *221*(1), 1–12. doi: 10.1243/09544097jrrt58.

Burrow, M. P. N., Ghataora, G. S., & Evdorides, H. (2011). Railway foundation design principles. *Journal of Civil Engineering and Architecture*, *5*(3), 224–232. doi: 10.17265/1934-7359/2011.03.003.

Chandra, S., & Agarwal, M. M. (2007). *Railway engineering* (p. 590). Oxford: Oxford University Press.

Chao, Z. (2014). Experimental study and constitutive modeling of cyclic behavior at small strains of unsaturated silt at various temperatures. Ph.D. Thesis. Hong Kong: University of Science and Technology.

Dareeju, B. S. (2017). Performance evaluation of unsaturated rail track foundations under cyclic moving wheel load. Ph.D. Thesis. Queensland University of Technology.

Fattah, M. Y., Al-Mosawi, M. J., & Al-Ameri, A. F. I. (2017). Dynamic response of saturated soil – foundation system acted upon by vibration. *Journal of Earthquake Engineering*, *21*(7), 1158–1188. doi: 10.1080/13632469.2016.1210060.

Fattah, M. Y., Mahmood, M. R., & Aswad, M. F. (2019). Stress distribution from railway track over geogrid reinforced ballast underlain by clay, earthquake engineering and engineering vibration. *Springer*, *18*(1), 77–93. doi: 10.1007/s11803-019-0491-z.

Fattah, M. Y., Mahmood, M. R., & Aswad, M. F. (2022). Stress waves transmission from railway track over geogrid reinforced ballast underlain by clay. *Structural Monitoring and Maintenance*, *9*(1), 1–27. doi: 10.12989/smm.2022.9.1.001.

Fattah, M. Y., Mahmood, M. R., & Aswad, M. F. (2024). Experimental and numerical settlement analysis of railway track over geogrid reinforced ballast. *Railway Sciences*, *3*(3), 311–331. doi: 10.1108/RS-11-2023-0042.

Fattah, M. Y., Majeed, Q. G., & Joni, H. H. (2024). Stresses in saturated and unsaturated subgrade layer induced by railway track vibration. *Infrastructures*, *9*(4), 64, doi: 10.3390/infrastructures9040064.

Feng, F., Luo, Q., Wang, T., Connolly, D. P., & Liu, K. (2024). Frequency spectra analysis of vertical stress in ballasted track foundations: Influence of train configuration and subgrade depth. *Transportation Geotechnics*, *44*, 101167. doi: 10.1016/j.trgeo.2023.101167.

François, B., & Laloui, L. (2008). ACMEG-TS: A constitutive model for unsaturated soils under non-isothermal conditions. *International Journal for Numerical and Analytical Methods in Geomechanics*, *16*(32), 1955–1988. doi: 10.1002/nag.712.

Gräbe, P. J. (2002). Resilient and permanent deformation of railway foundations under principal stress rotation. (PhD) thesis. University of Southampton.

Hayano, K., Ishii, K., & Muramoto, K. (2013). Effects of ballast thickness and tie-tamper repair on settlement characteristics of railway ballasted tracks. *The 18th International Conference on Soil Mechanics and Geotechnical Engineering* (pp. 1275–1282), Paris.

Jin, M. S., Lee, K. W., & Kovacs, W. D. (1994). Seasonal variation of resilient modulus of subgrade soils. *Journal of Transportation Engineering*, *120*(4), 603–616. doi: 10.1061/(asce)0733-947x(1994)120:4(603).

Lambe, T. W., & Whitman, R. V. (1969). *Soil mechanics*. New York: John Wiley & Sons.

Leshchinsky, B., & Ling, H. I. (2013). Numerical modeling of behavior of railway ballasted structure with geocell confinement. *Geotextiles and Geomembranes*, *36*, 33–43.

Li, D., & Selig, E. (1996). Cumulative plastic deformation for fine-grained subgrade soils. *Journal of Geotechnical Engineering*, *122*(12), 1006–1013. doi: 10.1061/(asce)0733-9410(1996)122:12(1006).

Li, X., Chen, Y., Zou, C., & Chen, Y. (2023). Train-induced vibration mitigation based on foundation improvement. *Journal of Building Engineering*, *76*(1), 107106. doi: 10.1016/j.jobe.2023.107106.

Li, D., Sussmann, T., Hyslip, J., & Chrismer, S. (2016). *Railway geotechnics*. Oxford: Taylor & Francis.

Loh, R. B. H., & Nikraz, H. (2012). Effective stress method on threshold stress of clay under high rate cyclic loading. In *Paper presented at the 5th Asia-Pacific Conference on Unsaturated Soils (AP-UNSAT 2011)*, Pattaya.

Mayne, P. W., Christopher, B. R., & DeJong, J. (2001). *Manual on subsurface investigations national highway institute publication No. FHWA NHI-01-031*. Washington, DC: Federal Highway Administration.

McCartney, J. S., & Khosravi, A. (2013). Field monitoring system for suction and temperature profiles under pavements. *Journal of Performance of Constructed Facilities*, *27*(6), 818–825. doi: 10.1061/(asce)cf.1943-5509.0000362.

Selig, E. T., & Waters, J. M. (1994). *Track geotechnology and substructure management*. London: Thomas Telford.

Sivakumar, V., Kodikara, J., O'Hagan, R., Hughes, D., Carins, P., & Mckinley, J. D. (2013). Effects of confining pressure and water content on performance of unsaturated compacted clay under repeated loading. *Geotechnique*, *63*(8), 628–640. doi: 10.1680/geot.10.p.103.

Tensar International. (2011). Brochre of Products.

Tripathy, S., Al-Khyat, S., Cleall, P. J., Baille, W., & Schanz, T. (2016). Soil suction measurement of unsaturated soils with a sensor using fixed-matrix porous ceramic discs. *Indian Geotechnical Journal*, *3*(46), 252–260. doi: 10.1007/s40098-016-0200-z.

Uchaipichat, A., & Khalili, N. (2009). Experimental investigation of thermo- hydro-mechanical behavior of an unsaturated silt. *Geotechnique*, *4*(59), 339–353.

Wichtmann, T., Andersen, K. H., Sjursen, M. A., & Berre, T. (2013). Cyclic tests on high-quality undisturbed block samples of soft Marine Norwegian clay. *Canadian Geotechnical Journal*, *4*(50), 400–412. doi: 10.1139/cgj-2011-0390.

Wu, L., & Shi, Z. (2023). Feasibility of vibration mitigation in unsaturated soil by periodic pile barriers. *Computers and Geotechnics*, *164*, 105798. doi: 10.1016/j.compgeo.2023.105798.

Yang, S. R., Lin, H. D., Kung, J. H. S., & Huang, W. H. (2008). Suction-controlled laboratory test on resilient modulus of unsaturated compacted subgrade soils. *Journal of Geotechnical and Geoenvironmental Engineering*, *134*(9), 1375–1384. doi: 10.1061/(asce)1090-0241(2008)134:9(1375).

Corresponding author
Mohammed Y. Fattah can be contacted at: myf_1968@yahoo.com